



# Surface renewal performance to independently estimate sensible and latent heat fluxes in heterogeneous crop surfaces



K. Suvočarev<sup>a,\*</sup>, T.M. Shapland<sup>b</sup>, R.L. Snyder<sup>c</sup>, A. Martínez-Cob<sup>a</sup>

<sup>a</sup> Department of Soil and Water, Estación Experimental Aula Dei (EEAD), CSIC, Avda. Montañana 1005, 50059 Zaragoza, Spain

<sup>b</sup> Department of Viticulture and Enology, University of California, Davis, CA 95616, USA

<sup>c</sup> Department of Land, Air and Water Resources, University of California, Davis, CA 95616, USA

## ARTICLE INFO

### Article history:

Received 16 July 2013

Received in revised form 4 November 2013

Accepted 16 November 2013

Available online 22 November 2013

This manuscript was handled by Konstantine P. Georgakakos, Editor-in-Chief, with the assistance of Matthew Rodell, Associate Editor

### Keywords:

Evapotranspiration

Eddy covariance

Surface renewal

Peach orchard

Energy balance

## SUMMARY

Surface renewal (SR) analysis is an interesting alternative to eddy covariance (EC) flux measurements. We have applied two recent SR approaches, with different theoretical background, that from Castellví (2004), SR<sub>Cas</sub>, and that from Shapland et al. (2012a,b), SR<sub>Shap</sub>. We have applied both models for sensible ( $H$ ) and latent (LE) heat flux estimation over heterogeneous crop surfaces. For this, EC equipments, including a sonic anemometer CSAT3 and a krypton hygrometer KH20, were located in two zones of drip irrigated orchards of late and early maturing peaches. The measurement period was June–September 2009. The SR<sub>Cas</sub> is based on similarity concepts for independent estimation of the calibration factor ( $\alpha$ ), which varies with respect to the atmospheric stability. The SR<sub>Shap</sub> is based on analysis of different ramp dimensions, separating the ones that are flux-bearing from the others that are isotropic. According to the results obtained here, there was a high agreement between the 30-min turbulent fluxes independently derived by EC and SR<sub>Cas</sub>. The SR<sub>Shap</sub> agreement with EC was slightly lower. Estimation of fluxes determined by SR<sub>Cas</sub> resulted in higher values (around 11% for LE) with respect to EC, similarly to previously published works over homogeneous canopies. In terms of evapotranspiration, the root mean square error (RMSE) between EC and SR was only 0.07 mm h<sup>-1</sup> (for SR<sub>Cas</sub>) and 0.11 mm h<sup>-1</sup> (for SR<sub>Shap</sub>) for both measuring spots. According to the energy balance closure, the SR<sub>Cas</sub> method was as reliable as the EC in estimating the turbulent fluxes related to irrigated agriculture and watershed distribution management, even when applied in heterogeneous cropping systems.

© 2013 Elsevier B.V. All rights reserved.

## 1. Introduction

Precision in sensible ( $H$ ) and latent heat (LE) flux estimation is important due to their great contribution to precipitation, plant growth, and the amount and locations of surface water runoff. Water use for irrigation purposes is the most important demand to be considered in watershed management. Irrigated agriculture should rely on evapotranspiration (ET) measurements. Together with increasing needs for more arable land and less water use per crop product, there has been a notable improvement in instrumentation, methods and approaches to estimate ET. In order to spread scientifically approved techniques into commercial practice, simpler approaches are preferred. Furthermore, in the absence of possibilities to apply direct measurements of turbulent fluxes such as eddy covariance (EC) or lysimeter measurements of ET

losses, surface renewal (SR) (Paw U et al., 1995) has been proposed as a reliable alternative ET estimation method.

The energy balance closure is used as a standard procedure to independently evaluate scalar flux estimates derived by micrometeorological methods (Wilson et al., 2002). Where closure is not achieved, flux measurements need to be interpreted to account for inconsistency with conservation principles (Kustas et al., 1999). Several reasons for the lack of closure of the surface energy budget in EC measurements have been discussed by Mahrt (1998): (1) lack of coincidence of the source areas (leaves and soil surface) among various flux components measured very near to a surface; (2) flux divergence arising from transport that is not one-dimensional such as insufficient fetch; (3) non-stationarity of the measured time series; (4) turbulent dispersive fluxes arising from organized planetary-boundary-layer circulations that may have preferred locations so that the mean vertical velocities at an instrument location may be systematically different from zero, hence giving rise to a vertical advective flux; and (5) systematic bias in instrumentation (Twine et al., 2000).

When using the SR method, some of the uncertainties related to EC instrumentation could be avoided: no orientation limitations,

\* Corresponding author. Tel.: +34 976716075.

E-mail addresses: [suvocarev@eead.csic.es](mailto:suvocarev@eead.csic.es) (K. Suvočarev), [tmshapland@ucdavis.edu](mailto:tmshapland@ucdavis.edu) (T.M. Shapland), [rlsnyder@ucdavis.edu](mailto:rlsnyder@ucdavis.edu) (R.L. Snyder), [macoan@eead.csic.es](mailto:macoan@eead.csic.es) (A. Martínez-Cob).

no leveling requirement, no shadowing or instrumentation separation issues, etc. Likewise, despite Castellví (2012) showed that in practice the fetch requirements for SR are similar as for the EC method, Castellví and Snyder (2009a) showed that the SR method can be operated at any height (roughness or inertial sublayer) and thus the SR is less stringent to the fetch requirements when a sonic anemometer is avoided. In other words, the SR equipment is more adjustable to the specific conditions of fetch (Castellví, 2012). Methodologically, SR is based on canopy layer turbulence and the time–space scalar field associated with the dominance of turbulent coherent structures. Numerous authors (Paw U et al., 1995; Snyder et al., 1996; Spano et al., 1997, 2000; Chen et al., 1997a,b; Castellví and Martínez-Cob, 2005; Zapata and Martínez-Cob, 2001; Zhao et al., 2010) have used a simple version of the SR method based on analyzing ramp-like patterns in the temperature time series to estimate  $H$ . It was proved to be applicable in a wide range of natural surfaces. In this case latent heat flux (i.e. ET expressed in energy terms) was obtained as the residue of the energy balance equation. Detailed theory behind the SR analysis basics and early advances are described in previous works by Paw U et al. (1995, 2005), Snyder et al. (1996), and Spano et al. (1997).

The main challenge facing the SR method is deriving the calibration factor ( $\alpha$ ), thus making SR dependent on other direct surface exchange measurements such as EC. According to some important studies in the topic (Paw U et al., 1995; Snyder et al., 1996; Katul et al., 1996; Duce et al., 1998; Castellví, 2004),  $\alpha$  for sensible heat flux depends on the measurement height, stability conditions, canopy architecture and size and design of the wire if thermocouples are used. When it comes to estimating  $\alpha$ , different explanations and methods have been proposed in order to derive repeatable procedures to correct the SR flux results. Namely, Paw U et al. (1995) proposed that the need for calibration arises from uneven coherent structure heating. Afterwards, Castellví (2004) proposed combining SR analysis with similarity theory to auto-calibrate SR, which requires also average wind speed measurements. One study over rice field demonstrated the feasibility of applying the Castellví ( $SR_{Cas}$ ) principles to independently derive  $H$  and  $LE$  (Castellví et al., 2006). Another study over rangeland grass used  $SR_{Cas}$  to estimate three scalar fluxes, demonstrating energy flux densities higher than the ones derived by the EC method: 4%, 18% and 10% for  $H$ ,  $LE$  and carbon dioxide ( $F_p$ ) fluxes, respectively (Castellví et al., 2008). Castellví et al. (2006, 2008) showed that this  $SR_{Cas}$  estimations improved energy balance closure when applied over homogeneous crop surfaces.

Recently, Shapland et al. (2012a, 2012b) proposed a SR method ( $SR_{Shap}$ ) for independent flux estimation by distinguishing the larger turbulent coherent structures responsible for the flux interchange from the smaller non-flux-bearing isotropic turbulence. Shapland et al. (2012b) applied this approach for the  $H$  estimation over bare soil, sorghum and teff grass fields. Their approach demonstrated that no calibration was needed under the unstable atmospheric conditions. Under the hypothesis that the smallest scale turbulent structures (Scale One) mix the larger scale coherent structures (Scale Two), which are responsible for direct energy and mass exchange,  $\alpha$  values are shown to be about 1.00.

To our knowledge, no other results have been reported on the application of the  $SR_{Cas}$  or  $SR_{Shap}$  approaches for calculating  $LE$  over heterogeneous canopies, where the turbulence can be enhanced by the presence of an uneven ground cover and the assumptions behind similarity theory may not be fulfilled. Thus, we have employed both  $SR_{Cas}$  and  $SR_{Shap}$  analyses in drip-irrigated peach orchards to estimate independently  $H$  and  $LE$  flux densities over the data collected by EC equipments. An EC installation was set up in each of two different peach orchards with distinct cultivars to provide a dataset to evaluate performance and applicability of the  $SR_{Cas}$  and  $SR_{Shap}$  methods over such a heterogeneous crop

surface when compared to EC values as a reference. The  $SR_{Cas}$  calculation requires high frequency temperature measurements and mean horizontal wind speed data. For  $SR_{Shap}$  calculation, only high-frequency scalar measurements are needed.

## 2. Materials and methods

### 2.1. Crop, site and instrumentation

Two EC stations were run from 1 June to 30 September 2009 at a commercial orchard La Herradura in Caspe (NE Spain, middle Ebro River Basin) to measure the surface energy balance components in two drip-irrigated peach orchards. The experimental site was characterized by relatively high winds (long-term annual average wind speed at 2 m above ground is  $3.1 \text{ m s}^{-1}$ ) and semiarid climate (long-term annual precipitation and reference evapotranspiration, 315 and 1392 mm, respectively) (Martínez-Cob and Faci, 2010).

The orchard was located next to a meander of the Ebro River, near to where the river forms a lake upstream of the Mequinenza dam (Fig. 1). The topography was rough, with elevation ranging from 120 to 200 m above the mean sea level (Fig. 2). Peaches represented 154 ha out of 227 ha total in the orchard. About 51 and 52 ha were cropped to early and late maturing peaches, respectively (Fig. 1). The remaining crops were cherries and apricots.

The first EC station (ST1) was set in a late peach zone ( $41^\circ 17' 40'' \text{ N}$  latitude,  $0^\circ 00' 24'' \text{ E}$  longitude), and the second EC station (ST2) was set in an early peach zone ( $41^\circ 18' 21'' \text{ N}$  latitude,  $0^\circ 00' 26'' \text{ E}$ ) (Fig. 1). Both late and early peach zones included several cultivars with similar phenological characteristics. Row orientation was north to south and canopy height was about 2.5 m for both orchards. The tree and row spacing were 3.75 m and 5.75 m for the late peaches, respectively, and 3.0 m and 5.0 m for the early peaches, respectively.

The soil down to 1.2 m depth was characterized by moderate to low average values of readily available water (70–110 mm) depending on the stoniness of a particular zone within the orchard (Zapata et al., 2013). Field capacity and wilting point were 0.29 and 0.13–0.14, respectively. Drip irrigation was applied daily. Two polyethylene irrigation laterals were used to irrigate each row of trees, one lateral at each side of the row. Turbulent (non-pressure compensating) emitters were used with a design discharge of  $41 \text{ l h}^{-1}$ . Emitters were extruded in the laterals at 1 m intervals. The discharge volume was  $24 \text{ l h}^{-1} \text{ tree}^{-1}$  for early peaches and  $30 \text{ l h}^{-1} \text{ tree}^{-1}$  for late peaches. Table 1 lists the monthly irrigation amounts during the measurement period. Due to their distinct phenological development (Table 2), late peaches received more irrigation water from June to September compared to the early peaches. Pruning and flower and fruit thinning practices were applied seasonally. Herbicides were applied to control weed growth and thus to minimize the presence of understory vegetation between the tree rows.

Both micrometeorological stations consisted of a sonic anemometer (Campbell Scientific, CSAT3), a krypton hygrometer (Campbell Scientific, KH20), a net radiometer (Kipp & Zonen, NR-Lite), an air temperature and relative humidity probe (Vaisala, HMP45C), four soil heat flux plates (Hukseflux, HFP01) and two soil temperature sensors (Campbell Scientific, TCAV). Two data loggers (Campbell Scientific, CR3000) were used to monitor these different sensors. All instruments except the soil sensors were placed on the top of a tower, at  $z = 6.9 \text{ m}$  above the ground. The sonic anemometers were placed pointing towards the northwest, about  $315^\circ$  from north clockwise in late peaches and  $308^\circ$  from north clockwise in early peaches, as this is the most predominant wind direction in the middle Ebro River area (Martínez-Cob et al., 2010). In addition, a previous study of the wind rose recorded at a nearby

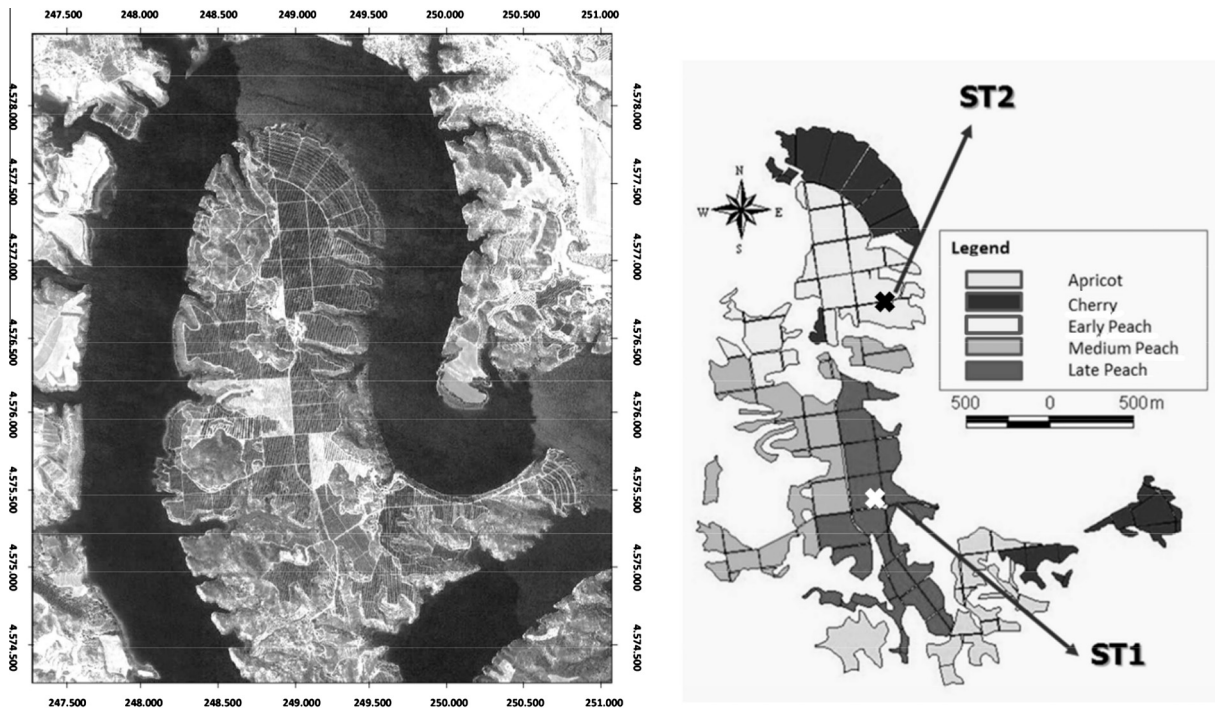


Fig. 1. Location of the two micrometeorological stations at the commercial orchard La Herradura.

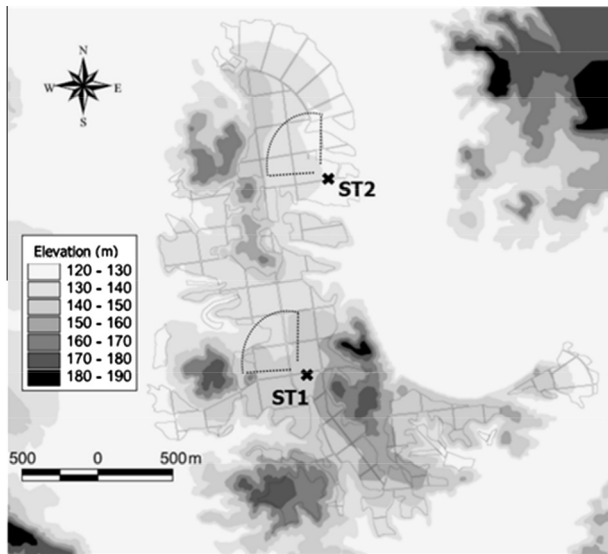


Fig. 2. Topography of the study orchards and measurements' spots location. Dotted line are rough presentation of the footprint, with radius equal to minimum fetch requirement (377 m).

standard weather station for 2004 to 2008 (June–September) showed also a similar predominant wind direction. The Krypton hygrometers were installed at about 16 cm horizontal distance from the west side of the CSAT3, slightly shifted behind it relative

to the prevailing wind direction. The net radiometers were placed oriented towards south. Soil heat flux plates were buried at 0.1 m depth, two in between rows and the other two in the row. Each soil temperature probe had four thermocouples (chromel-constantan), buried into pairs at 0.03 m and 0.06 m depth above each soil heat flux plate.

The 10 Hz raw data included wind speed at the  $x$  ( $u$ ) and  $y$  ( $v$ ) horizontal axes and at the  $z$  ( $w$ ) vertical axis, sonic temperature ( $T_s$ ), and vapor density [ $Q$ , recorded as the natural logarithm of the sensor voltage output according to the KH20 krypton hygrometer specifications (Campbell Scientific, 1996)], as well as air temperature ( $T_a$ ) and relative humidity (RH) recorded from the Vaisala probes. The loggers also recorded 10 Hz values of net radiation ( $R_n$ ), soil heat flux plate values and soil temperature, and the corresponding 30-min averages were stored. The recorded soil heat flux values were corrected as described by Allen et al. (1996) using the soil temperature records to get soil heat flux in the soil surface layer. Thus, at each 30-min period, the four soil heat flux values obtained were averaged to get a single value of soil heat flux ( $G$ ).

During the experiment planning stage it was necessary to roughly estimate the best position for setting our measurement equipment as we had to take into account the topographic variability and the irregular shape of the orchards (Figs. 1 and 2). Therefore a rough estimation of fetch requirements and the fraction  $F$  of scalar fluxes detected from within the fetch were performed. Allen et al. (1996) suggested using the theoretical considerations of boundary layer development to estimate minimum fetch requirements depending on surface roughness as:

Table 1  
Monthly irrigation and precipitation amounts during the measurement periods.

	Maturing type	June	July	August	September	Total
Irrigation (mm)	Late	88.8	116.8	87.1	88.6	494.3
	Early	147.3	94.9	57.0	29.9	442.1
Precipitation (mm)		25.6	24.8	30.4	32.2	113.0

**Table 2**  
Phenology of the studied peach cultivar types.

Maturity type	Blooming	Pit hard	Harvest begins	Harvest ends	Leaf fall
Late	13-Mar	14-Jun	13-Sep	06-Oct	15-Nov
Early	03-Mar	06-May	18-Jun	27-Jun	30-Oct

$$x_f = \left( \frac{30(z-d)}{z_{om}^{0.125}} \right)^{1.14} \quad (1)$$

where  $x_f$  (m) is the minimum fetch distance required for complete boundary development,  $z$  (m) is the measurement height above the ground,  $d$  (m) is zero-plane displacement and  $z_{om}$  (m) is momentum roughness height of the surface ( $0.123^*h$ ). This equation is valid for near-neutral conditions. Under stable conditions the exponent 1.14 should be increased, while it should be decreased under unstable conditions (Allen et al., 1996). Consequently, fetch requirements are shorter in case of unstable atmospheric conditions than those from Eq. (1). The experimental orchards were surrounded by the same or similar species of trees, so the boundary development was not limited by big changes in the surface roughness (Figs. 1 and 2).

Once the fetch distance was estimated, the fraction  $F$  of the scalar fluxes coming from within the aimed distance was calculated using the following equation from Allen et al. (1996):

$$F = \exp \left( \frac{(z-d)(1 - \ln((z-d)/z_{om})) - z_{om}}{k^2 x_f \left(1 - \frac{z_{om}}{(z-d)}\right)} \right) \quad (2)$$

where  $F$  is a fraction of  $H$  or  $LE$  density at the measurement height ( $z$ ) coming from the fetch distance ( $x_f$ ). Eq. (2) overestimates  $F$  for stable conditions and underestimates it under unstable conditions.

## 2.2. Micrometeorological methods and data processing

Calculations of fluxes were done over data sets that were previously corrected for: (1) two-dimensional coordinate rotation of the three wind speed components; (2) the lag between the vertical wind speed and the temperature data; (3) despiking (discarding values higher or lower than 4 standard deviations from the mean) the virtual temperature and water vapor concentration data. Additionally,  $LE$  fluxes were corrected for (1) the oxygen concentration as it affects the Krypton hygrometer and (2) the effect of the density variation due to the heating of air parcel and volume changes, i.e. the Webb-Pearman-Leuning correction (Webb et al., 1980). Corrected data were subsequently led through processing for calculating 30-min turbulent fluxes. For EC procedure, the fluxes,  $H_{EC}$  and  $LE_{EC}$ , were calculated both in  $W m^{-2}$ :

$$H_{EC} = \overline{\rho_a} \overline{C_p} \overline{w' T'_s} \quad (3)$$

$$LE_{EC} = \frac{\overline{\lambda} \overline{w' Q'}}{xKw} \quad (4)$$

where the overbar and the apostrophe denote 30-min averages and fluctuations around the mean, respectively;  $\overline{\rho_a}$  ( $kg m^{-3}$ ) is mean air density;  $\overline{C_p}$  ( $J kg^{-1} K$ ) is the specific heat of the air;  $\overline{w' T'_s}$  is the covariance between  $w$  ( $m s^{-1}$ ) and  $T_s$  ( $^{\circ}K$ ),  $\overline{\lambda}$  ( $J g^{-1}$ ) is the latent heat of vaporization;  $\overline{w' Q'}$  is the covariance between  $w$  and  $Q$  ( $\ln(mV)$ ), and  $xKw$  ( $\ln(mV) m^3 g^{-1}$ ) is the factory calibration factor of the krypton hygrometer (used to obtain water vapor density in terms of  $g m^{-3}$ ).  $\overline{\rho_a}$ ,  $\overline{C_p}$  and  $\overline{\lambda}$  were the 30-min averages of the 10 Hz values of  $\rho_a$ ,  $C_p$  and  $\lambda$  computed from the raw data of  $T_a$  and RH. This 30-min time frame was used because for that period of time stationarity conditions in agricultural surfaces are met and  $SR_{Cas}$

analysis relies on the similarity-based relationships determined for half-hour samples (Castellví and Snyder, 2010).

The  $SR_{Cas}$  analysis was performed using the same high frequency data with the corrections required for EC. By analyzing the scalar time series with multiple orders of structure functions, as proposed by Van Atta (1977), it is possible to derive the repetition frequency of coherent structures renewing the surface layer, the amplitude of the scalar ramps, and the surface exchange estimates (Paw U et al., 2005; Snyder et al., 1996). Castellví et al. (2006, 2008) have applied these structure functions from Van Atta (1977) to determine the ramp amplitude, but used the Chen et al. (1997b) approach for the ramp duration. Here we have decided to stick to Van Atta (1977) approach for both the ramp amplitude and duration:

$$S^n(j) = \frac{1}{m-j} \sum_{i=1+j}^m (V_i - V_{i-j})^n \quad (5)$$

where  $V_i$  and  $V_{i-j}$  are high-frequency measurements of either air temperature or water vapor density between two sequential time lags;  $j$  is the sample lag interval;  $m$  is the number of data points in the 30-min time period;  $i$  is the summation index; and  $n$  is the structure function order. Van Atta (1977) showed that the modeled ramp amplitude can be obtained by solving for the real roots of the following cubic equation:

$$y = A^3 + pA + q \quad (6)$$

where the coefficient for the linear term,  $p$ , is determined from the structure functions as follows:

$$p = 10S^2(j) - \frac{S^5(j)}{S^3(j)} \quad (7)$$

and the coefficient for the offset term,  $q$ , is determined solely by the third order structure function:

$$q = 10S^3(j) \quad (8)$$

Finally, the ramp duration can be found as:

$$\tau = -\frac{A^3 j}{S^3(j)} \quad (9)$$

It is possible to derive the  $SR_{Cas}$  scalar fluxes, sensible ( $H_{SR_{Cas}}$ ) and latent heat fluxes ( $LE_{SR_{Cas}}$ ), both in  $W m^{-2}$ , at measuring height  $z$  (m) by using the ramp characteristics, ramp amplitude and ramp duration (Paw U et al., 1995; Castellví et al., 2006).

$$H_{SR_{Cas}} = z \overline{\rho_a} \alpha_T \overline{C_p} \frac{A_T}{\tau_T} \quad (10)$$

$$LE_{SR_{Cas}} = z \alpha_q \lambda \frac{A_q}{\tau_q} \quad (11)$$

again,  $z$  is 6.9 m in our case;  $\alpha$  is the calibration factor; indexes  $T$  and  $q$  are to distinguish the ramp dimensions for  $H$  and  $LE$ , respectively.

To estimate the non-dimensional  $\alpha$  factor, the one-dimensional diffusion equation with SR analysis and similarity concepts were combined into the following equation valid for the scalars being measured within the inertial sublayer (Castellví, 2004):

$$\alpha = \left[ \frac{k}{\pi} \frac{(z-d)}{z^2} \tau u \phi^{-1}(\xi) \right]^{1/2} \quad (12)$$

where  $k \sim 0.4$  is the von Kármán's constant;  $d$  (m) is the zero-plane displacement;  $u_*$  ( $\text{m s}^{-1}$ ) is the friction velocity;  $\phi(\xi)$  is the stability function for scalar transport; the stability parameter  $\xi$  is defined as  $(z-d)/L_0$ , where  $L_0$  (m) is the Obukhov length. Namely, application of stability functions by Castellví (2004) in deriving the  $H$  and LE resulted in improved energy balance closure. No scalar exchange was assumed through the top of the air parcel, therefore, vertical and horizontal advection was neglected (Castellví et al., 2006).

In the summary of the SR method and its applications by Paw U et al. (2005), it is explained that the SR method applies in both the roughness and inertial sublayer. The equations for  $\alpha$  value calculation employed in this work were considered for the measurements made in the inertial sublayer. Following Sellers et al. (1986), the bottom of the inertial sublayer may be estimated as  $z^* = h + 2(h-d) \sim 5/3h$  when  $d = 2/3h$ . In our case, counting with 2.5 m canopy height,  $z^*$  was calculated to be  $\sim 4.2$  m above ground. Although in some cases under unstable conditions the bottom of inertial sublayer was found to be up to 4 times the crop height (Castellví and Snyder, 2009b), we believe that our measurements at  $z = 6.9$  m were well inside the inertial sublayer for most of the data.

The Obukhov length  $L_0$  was calculated by:

$$L_0 = - \frac{\bar{T}_s u_*^3}{kgw'T_s} \quad (13)$$

where friction velocity was calculated as the square root of covariance between rotated vertical and horizontal wind components (Stull, 1988):  $u = \sqrt{u'w'}$ .

The stability functions were assumed to be universal for both scalars. They are defined by Foken (2006) and Höglström (1988) as:

$$\phi(\xi) = \begin{cases} (0.95 + 7.8\xi) & 0 \leq \xi \leq 1 \\ 0.95(1 - 11.6\xi)^{-1/2} & -2 \leq \xi < 0 \end{cases} \quad (14)$$

From the invoked assumptions, Eq. (12) is valid when measurements are made over homogeneous canopies and stationary conditions apply during the sampling period, which is typically about half an hour, since dominant energy term in the surface energy balance, net radiation, does not change significantly for such a short period of time. It has been shown that the equation worked well in homogeneous short plant canopies. We have applied the same equations on the sparse orchard grove with peach trees to evaluate both  $H_{\text{SRCas}}$  and  $LE_{\text{SRCas}}$  estimation.

The structure functions from Van Atta (1977) imply that the surface layer exchange for the stationary period of time is represented with repeating number of ramps that are of the same dimension. Shapland et al. (2012a,b) warn that it is important to identify ramps of different dimension to estimate the efficiency of coherent structures in transporting mass and momentum, which is influenced by the detection scheme (Antonia et al., 1983; Gao et al., 1989; Collineau and Brunnet, 1993). By expanding structure function analysis to identify two ramp scales, the difference between the smallest coherent structure with “intermittent” gradual rise ramp period and the dominant coherent structure characterized by “persistent” gradual rise ramp period is defined (Shapland et al., 2012a,b). The idea is that the method should consider only the ramp scales that are responsible for the surface-layer exchange (Scale Two) and therefore calculate direct fluxes that do not need calibration. The short duration, Scale One ramps are treated as instantaneous events of mixing air to uniform air parcel heating while residing in the canopy that will later be ejected to atmosphere. Shapland et al., (2012a,b) showed that the dominant ramp scale is actually bearing the surface layer exchange, when it is

applied over bare ground and short canopies under unstable conditions.

The method first uses the Van Atta (1977) procedure to obtain the Scale One ramp amplitude, ramp period and gradual rise period. Next, the Scale One gradual rise period is compared to the Scale One ramp period to classify its magnitude by using the gradual rise duration as the criterion. If it is shorter than the half of the ramp period, the scale of that event is considered intermittent. In that case, time lag is set equal to Scale One gradual rise period in order to filter it out, and Van Atta procedure is further applied to obtain the Scale Two ramp characteristics. Otherwise, for the longer gradual rise periods that occupy the major part of the ramp period, the ramp is considered as persistent. Then, the calculation of the Two Scale ramp characteristics is done by setting the time lags to be half of the Scale One ramp period. In this way, the Scale One is included in calculation procedure and is identified as the bigger-persistent Scale. By using Two Scale ramp characteristics, the expressions for calculating fluxes are similar to the classical surface renewal, but without  $\alpha$ , as it is considered to be  $\sim 1.00$ .

$$H_{\text{SRShap}} = z \bar{\rho}_a \bar{C}_p \frac{A_{T2}}{\tau_{T2}} \quad (15)$$

$$LE_{\text{SRShap}} = z \bar{\lambda} \frac{A_{q2}}{\tau_{q2}} \quad (16)$$

All calculation procedures were performed using R software (R Development Core Team, 2012).

Micrometeorological stations were mounted in a way that footprint in the prevailing wind direction was within the same peach plots. Because of the topography and the irregular shape of the studied plots, we only analyzed those 30-min periods for which wind was between  $\pm 45^\circ$  of the angle to which sonic anemometers were pointing,  $308^\circ$  for late and  $315^\circ$  for early peaches (Fig. 2).

### 2.3. Data analyses

The performance and energy balance closure of the three methods, EC,  $SR_{\text{Cas}}$ , and  $SR_{\text{Shap}}$  were evaluated using linear regression analysis and root square mean error, RSME, (e.g. Jamieson et al., 1998). Furthermore, the ratio  $D = \Sigma y / \Sigma x$ , where  $\Sigma y$  were the SR fluxes or, for energy balance closure evaluation, the  $LE + H$  fluxes, while  $\Sigma x$  were the EC fluxes or, for energy balance closure evaluation, the  $Rn - G$  term.  $D$  was calculated to easily express under- or over-estimation of the energy balance or simply to compare scalar fluxes derived by the different methods (Castellví and Snyder, 2010).

## 3. Results and discussion

The general meteorological conditions at the two sites are listed in Table 3. Little difference was noticed. Mean monthly air temperatures were higher in July and August. Rainfall was small during the experiment and the most important rain events occurred in

**Table 3**

General mean monthly meteorological conditions within the experimental period recorded at the two measurement spots, late maturing (ST1) and early maturing (ST2) peaches: T, air temperature; VPD, air vapor pressure deficit; WV, wind velocity.

	T (°C)		VPD (kPa)		WV (m s <sup>-1</sup> )	
	ST1	ST2	ST1	ST2	ST1	ST2
June	24.1	24.2	1.2	1.2	2.3	2.1
July	25.8	26.0	1.2	1.3	2.7	2.5
August	25.9	26.3	1.1	1.1	2.0	2.0
September	21.2	21.5	0.7	0.7	2.0	1.9

September (Table 1). Vapor pressure deficit was higher for the hotter and drier months. This is a windy area with recorded mean monthly wind velocities, for the experimental season, between 1.9 and 2.7 m s<sup>-1</sup>. The wind roses for the year 2009 at ST1 and ST2 showed slightly different wind direction distribution between both micrometeorological sites probably due to difference in the measuring site elevations and therefore ST1 being more exposed to winds; less calm winds were observed at ST1 (21.7%) than at ST2 (26.1%). Predominant wind directions were west or east (ST1) or west or east to southeast (ST2). East to southeast winds were considered as ‘bad wind direction data’ as discussed previously and its relatively high frequency led to the removal of more data (about half of total data recorded) than expected according to the general wind direction distributions in the middle Ebro river (Martínez-Cob et al., 2010) and the wind rose for the nearby weather station.

The SR<sub>Cas</sub> estimated  $\alpha$  values with respect to stability function for four cases ( $\alpha_T$  and  $\alpha_q$  for both stations, ST1 and ST2) are represented in Fig. 3. Most of the values were found between 0.25 and 1.5; those for unstable conditions were higher (0.5–1.5) than those obtained for stable conditions (0.25–1.0). The values for unstable conditions had greater variability than those for stable atmospheric conditions, which tend to have more uniform value under very stable conditions ( $\alpha < 0.25$ ). The uniformity for the stable cases may be because both scalar fluxes were low, so the calibration value was lower and it tended to a constant value. It can be assumed that stationary characteristics for the summer nocturnal conditions in this area also contribute to that small variation in  $\alpha$  values. As Eq. (12) indicates, the  $\alpha$  value is directly dependent on the ramp duration and friction velocity and it is inversely proportional to  $\phi(\zeta)$ . Therefore, it was expected to obtain higher and more variable  $\alpha$  values for the unstable conditions when more variability is usual for the daytime parameters. When averaged all values for the stable periods during the measuring season, we have got similar values for  $\alpha_T$  and  $\alpha_q$  at both sites (0.40–0.47). For unstable periods similar values were found at each site, 0.70 and 0.72 for  $\alpha_T$  and 0.53 and 0.56 for  $\alpha_q$ . Nevertheless, the implications of  $\alpha$  value are still not well understood, especially under the stable atmospheric conditions (Castellví, 2004).

Shapland et al. (2012a) hypothesized that while ramp gradual rise periods of Scale One are much shorter than those of Scale Two, ramp amplitudes of Scales One and Two are approximately the same. Therefore, it is expected that  $\alpha$  is less than 1.00 when the Scale One is used in calculation procedure and calibration is necessary, which was seen in the classical SR application. Following the new two Scale model, only the flux-bearing Scale Two structure functions are considered and therefore it is expected that calibration is avoided. Shapland et al. (2012b) argued that the method is not performing satisfactory when some of the assumptions behind the method’s theory are violated and then calibration might be needed. Namely, the most probable misleading assumption is the existence of only Two Scales of ramps. Besides, in the same paper the authors state that for the intervals during which the Scale One ramp period is more than 0.5 of the Scale Two ramp period the expanded Van Atta (1977) procedure is not as effective at resolving the ramp characteristics of Scale Two, making the Scale Two surface renewal H estimations less accurate.

According to Eq. (1), the minimum fetch requirements for near-neutral conditions in this experiment should be  $x_f = 377$  m for complete boundary development. For that distance the estimated fraction of the H and LE fluxes coming from the targeted canopy, according to Eq. (2), would be  $F = 85\%$ . Relaxed fetch requirements have been stated for the SR method. As discussed earlier, it can be used at variable heights with respect to canopy, i.e. inside the roughness or inertial layer (Paw U et al., 1995; Castellví and Snyder, 2009a). Also, SR sensors can be mounted at a lower heights than EC instruments to allow the footprint to be well inside the area of interest and to maximize the data collection amount and quality. Nevertheless, in this particular work, we believe that the same fetch requirements rules apply for both EC and SR when CSAT3 is used and measurements for both methods are taken at the same level inside the inertial sublayer, which was explained by Castellví (2012).

Due to the similarity assumptions in the SR<sub>Cas</sub> method, the monthly averages of the half-hour values of SR<sub>Cas</sub> ramp duration ( $\tau$ ) obtained for both H and LE at both sites were compared (Fig. 4). For each particular month, these mean values represent the average evolution of  $\tau$  along a 24-h period for each month.

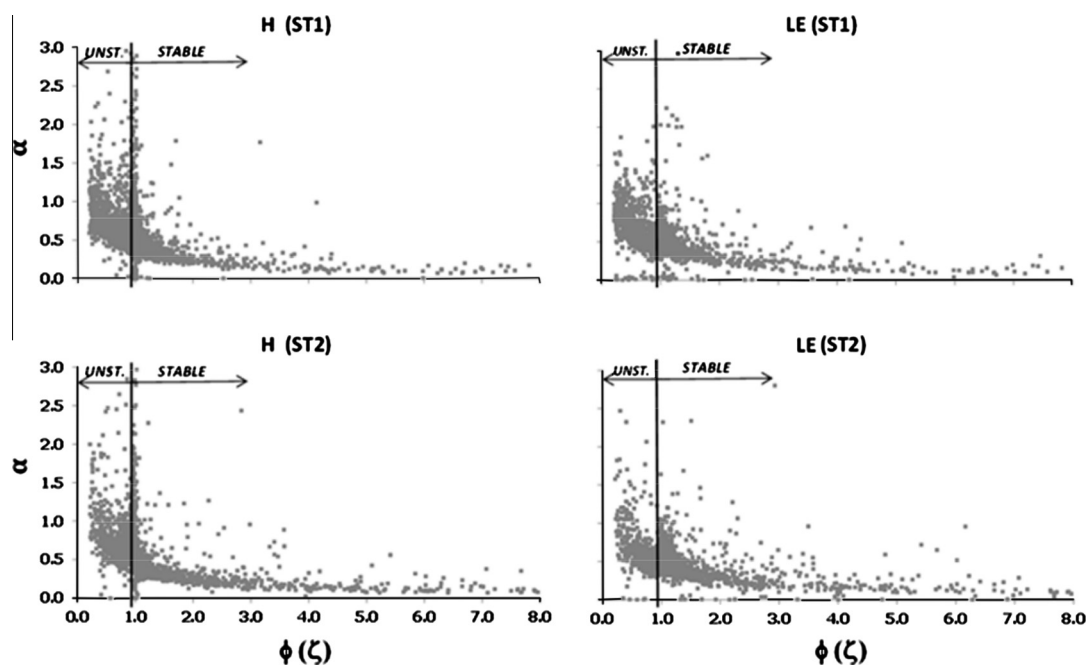


Fig. 3. Surface renewal Castellví approach (SR<sub>Cas</sub>) calibration factor ( $\alpha$ ) for both latent (LE) and sensible (H) heat flux estimation with respect to stability function ( $\phi(\zeta)$ ). ST1, station located at late maturing peaches; ST2, station located at early maturing peaches.

There was strong agreement found between  $\tau$  values obtained for both scalar fluxes,  $H_{\text{SRCas}}$  and  $LE_{\text{SRCas}}$ , under both stable and unstable conditions. At the ST1, worse agreement in  $\tau$  for both scalars was obtained for August when some values of  $\tau$  differed by 100–200 s or more. The ST2 datasets for  $\tau$  had more noise but were also in agreement when the highest peaks are disregarded. The SR theory is based on the contact time of air coherent structure with plant canopy and corresponding dispersive processes of temperature (or other scalar) exchange (Paw U et al., 1995). Under stable atmospheric conditions, a few minutes can be considered the lifespan of a coherent structure (Gao et al., 1989). Thus, when few minutes is the difference between the ramp durations associated with each scalar, the similarity between heat and water vapor transport by the turbulent air flow may not apply. Some of the higher peaks can be considered as noise, although we attempted to filter out data in order to avoid uncertainty introduced by the results obtained under unfavorable conditions with low levels of turbulence. We can see from Fig. 4 that the disagreement between  $\tau$  calculated for the  $H_{\text{SRCas}}$  and  $LE_{\text{SRCas}}$  may occur during both stable and unstable atmospheric conditions.

Relatively poor performance of both  $\text{SR}_{\text{Shap}}$  and  $\text{SR}_{\text{Cas}}$  methods was observed for estimation of  $H$  and  $LE$  for stable atmospheric conditions (Table 4). Thus, the computed  $R^2$  values for stable ( $0 < \zeta < 1$ )  $H$  data comparisons between EC and surface renewal methods,  $\text{SR}_{\text{Cas}}$  and  $\text{SR}_{\text{Shap}}$ , were relatively low, 0.32 and 0.28 (late peaches) and 0.45 and 0.35 (early peaches), respectively. For the  $LE$  data under the same atmospheric conditions, the comparison between EC and  $\text{SR}_{\text{Cas}}$  and  $\text{SR}_{\text{Shap}}$ , reported higher  $R^2$  values, 0.48 and 0.60 (late peaches) and 0.63 and 0.67 (early peaches), respectively. In terms of the  $D$  statistics, the SR methods gave higher values than EC fluxes.  $H_{\text{SRCas}}$  were about 39% (late peaches) and 18% (early peaches) higher and  $H_{\text{SRShap}}$  were about 96% (late peaches) and 104% (early peaches) higher for stable atmospheric conditions. For  $LE_{\text{SRCas}}$  that overestimation was lower, about 11% for both late and early peaches and for  $LE_{\text{SRShap}}$  they were around 40% and 31%, respectively.

Under unstable atmospheric conditions ( $-2 < \zeta < 0$ ) less overestimation was observed, but still SR analysis resulted in higher  $D$  values in almost all cases. Namely, values for  $H_{\text{SRCas}}$  were 6% and 9% higher than  $H_{\text{EC}}$  and  $H_{\text{SRShap}}$  6% higher and 4% lower;  $LE_{\text{SRCas}}$  were 11% and 12% and  $LE_{\text{SRShap}}$  10% and 11% higher than the  $LE_{\text{EC}}$ .  $R^2$  under the same conditions was very high for  $H_{\text{SRCas}}$  (0.83 and 0.88) and less for  $H_{\text{SRShap}}$  (0.66 and 0.60), also for  $LE_{\text{SRCas}}$  (0.76 and 0.86) and less for  $LE_{\text{SRShap}}$  (0.46 and 0.49).

When we compared  $H$  and  $LE$  data between the EC and  $\text{SR}_{\text{Cas}}$  methods for all atmospheric conditions, agreement was very high as the regression slopes were close to 1.0 (but significantly

different from 1.0, level of significance of 0.05) and the intercepts and RMSE were small (Table 4). The different statistics used indicate that  $\text{SR}_{\text{Cas}}$  performed better in estimating the  $H$  than  $LE$  fluxes. There are no clear reasons why  $\text{SR}_{\text{Cas}}$  performed different in estimating  $H$  and  $LE$  values. We agree with explanations given by Castellví et al. (2008) that one possible source of error may lie in correction implemented for unaccounted density variations in incompressible flow. Namely, the WPL correction is sensitive to the propagation of errors stemming from scalar covariance estimation. Nevertheless, when calculating  $\text{SR}_{\text{Cas}}$  fluxes without applying WPL, the results only changed by few percent (data not shown).

The  $\text{SR}_{\text{Shap}}$  method showed differences in estimating  $H$  and  $LE$  fluxes but there was not a clear pattern. We believe that in this case, the data gaps were responsible for inconsistency in the statistics. Scale Two surface renewal data were omitted if the values were unreasonable. The unreasonable values likely arise from poor resolution of the Scale Two ramp characteristics, which occurs when the assumptions behind the expanded Van Atta (1977) method described in Shapland et al. (2012a) are violated. Namely, the variability in the number of datasets obtained for stable or unstable atmospheric conditions possibly influences the statistics to give different measures of agreement.

Energy balance closure results for stable, unstable and all atmospheric stability conditions for EC,  $\text{SR}_{\text{Cas}}$  and  $\text{SR}_{\text{Shap}}$  are listed in Table 5. As expected for  $\text{SR}_{\text{Cas}}$  better performance is noticed for unstable conditions than for stable conditions.  $\text{SR}_{\text{Cas}}$  analysis resulted in similar or even slightly better energy balance closure than EC, according to the statistical parameters listed. Statistics from Table 5 for all stability conditions for  $\text{SR}_{\text{Shap}}$  performance are indicating that there was high correlation (with  $R^2$  of 0.81 and 0.80 for early and late peaches, respectively) between  $\text{Rn-G}$  and  $\text{SR}_{\text{Shap}}$  flux results although it was lower than the one observed in EC and  $\text{SR}_{\text{Cas}}$  analysis. RMSEs showed also poorer performance, especially considering the number of data points analyzed. These results for the  $\text{SR}_{\text{Shap}}$  should be taken with caution due to the limited amount of data points yielded.

For the case inclusive of all atmospheric stability conditions, the statistics  $D$  indicates that only 6% (late peaches) and 2% (early peaches) of energy was underestimated by turbulent fluxes derived by the  $\text{SR}_{\text{Cas}}$  approach on the seasonal level (Table 5). Slightly poorer performance was observed in case of  $\text{SR}_{\text{Shap}}$  approach with 10% and 13% of lack of energy balance closure. EC results showed 13% (ST1) and 12% (ST2) of flux lost in energy balance for all data of the season. The lack of the energy balance closure of 12% and 13% is within earlier reported results for EC measurements over different plant canopies (Wilson et al., 2002). The figures of 6% and 2% energy imbalance for the  $\text{SR}_{\text{Cas}}$  method are in agreement

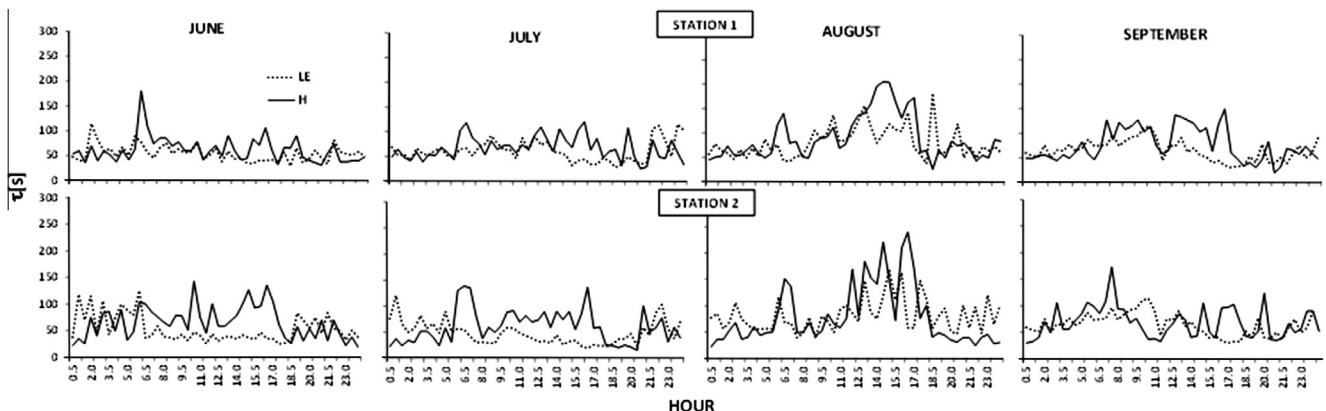


Fig. 4. Monthly averages of the 30-min values of ramp duration ( $\tau$ ) for the sensible (solid line) and latent (dotted line) heat fluxes obtained by the Surface renewal Castellvi approach ( $\text{SR}_{\text{Cas}}$ ) during the 4 months of the experimental measurement period. Station 1 at late peach spot; Station 2 at early peach spot.

**Table 4**  
Comparison between eddy covariance sensible and latent heat fluxes ( $H_{EC}$  and  $LE_{EC}$ ) and the corresponding fluxes derived by the surface renewal method in two peach maturing types: (a) following Castellví et al. (2006, 2008) ( $H_{SRCas}$  and  $LE_{SRCas}$ ), (b) following Shapland et al. (2012a,b) ( $H_{SRShap}$  and  $LE_{SRShap}$ ).  $H_{EC}$  and  $LE_{EC}$  were considered as independent variable ( $x$ ) for regression analysis.  $b_1$ , regression slope;  $b_0$ , regression intercept;  $R^2$ , coefficient of determination; RMSE, root mean square error;  $D$ , ratio of total sums ( $\Sigma y/\Sigma x$ ),  $N$ , number of values available; Var., variable.

Peach	Var. $x$	Var. $y$	Stability	$b_1$	$b_0$ ( $W m^{-2}$ )	$R^2$	RMSE ( $W m^{-2}$ )	$D$	$N$
Late	$H_{EC}$	$H_{SRCas}$	Stable	0.76	-13.67	0.32	19.93	1.39	984
			Unstable	1.04	1.16	0.83	25.85	1.06	1062
			All	0.93	0.04	1.00	23.19	0.93	2046
	$H_{EC}$	$H_{SRShap}$	Stable	1.02	-18.44	0.28	40.07	1.96	412
			Unstable	1.16	-8.26	0.66	45.96	1.06	436
			All	1.20	-12.97	0.79	42.27	0.80	848
	$LE_{EC}$	$LE_{SRCas}$	Stable	0.61	17.67	0.48	45.60	1.11	958
			Unstable	0.94	29.35	0.76	51.47	1.11	1047
			All	0.96	16.10	0.82	48.75	1.11	2005
	$LE_{EC}$	$LE_{SRShap}$	Stable	1.26	4.58	0.60	53.05	1.40	636
			Unstable	0.93	31.21	0.46	93.32	1.10	418
			All	1.04	12.06	0.68	71.78	1.17	1054
Early	$H_{EC}$	$H_{SRCas}$	Stable	0.99	-5.28	0.45	19.75	1.18	1016
			Unstable	1.07	1.91	0.88	21.70	1.09	789
			All	1.10	-1.47	0.92	20.62	1.01	1805
	$H_{EC}$	$H_{SRShap}$	Stable	1.67	-10.78	0.35	49.88	2.04	262
			Unstable	0.99	-1.85	0.60	39.15	0.96	334
			All	1.19	-20.88	0.79	44.19	0.53	596
	$LE_{EC}$	$LE_{SRCas}$	Stable	0.90	7.47	0.63	43.00	1.11	964
			Unstable	1.04	16.66	0.86	49.34	1.12	717
			All	1.05	6.70	0.88	45.81	1.12	1681
	$LE_{EC}$	$LE_{SRShap}$	Stable	1.19	4.19	0.67	44.24	1.31	522
			Unstable	1.08	6.44	0.49	111.74	1.11	284
			All	1.09	6.30	0.73	75.28	1.16	806

**Table 5**  
Energy balance closure performance for the (a) eddy covariance (subscripts'EC), (b) surface renewal following Castellví et al. (2006, 2008) (subscripts'SRCas) and (c) surface renewal following Shapland et al. (2012a,b) (subscripts'SRShap) estimated fluxes at two different peach maturing type spots. Available energy (Rn-G) was considered as independent variable ( $x$ ) to be compared to the sum of turbulent fluxes ( $H + LE$ ) variable ( $y$ ) in regression analysis.  $b_1$ , regression slope;  $b_0$ , regression intercept;  $R^2$ , coefficient of determination; RMSE, root mean square error;  $D$ , ratio of total sums ( $\Sigma y/\Sigma x$ ),  $N$ , number of values available; Var., variable.

Peach	Var. $x$	Var. $y$	Stability	$b_1$	$b_0$ ( $W m^{-2}$ )	$R^2$	RMSE ( $W m^{-2}$ )	$D$	$N$
Late	(Rn-G) <sub>EC</sub>	(H + LE) <sub>EC</sub>	Stable	0.66	18.94	0.50	53.65	-1.31	983
			Unstable	0.74	19.63	0.76	95.74	0.81	1059
			All	0.74	20.33	0.87	78.35	0.87	2042
	(Rn-G) <sub>SRCas</sub>	(H + LE) <sub>SRCas</sub>	Stable	0.61	14.77	0.50	51.17	-0.94	957
			Unstable	0.72	51.80	0.61	104.05	0.89	1046
			All	0.78	24.27	0.82	83.09	0.94	2003
	(Rn-G) <sub>SRShap</sub>	(H + LE) <sub>SRShap</sub>	Stable	1.07	11.77	0.71	53.16	-2.85	326
			Unstable	0.84	4.30	0.51	121.09	0.86	269
			All	0.85	7.51	0.80	90.91	0.90	595
Early	(Rn-G) <sub>EC</sub>	(H + LE) <sub>EC</sub>	Stable	0.76	8.76	0.87	30.81	-2.54	958
			Unstable	0.84	-0.91	0.88	72.74	0.84	714
			All	0.81	8.67	0.96	52.95	0.88	1672
	(Rn-G) <sub>SRCas</sub>	(H + LE) <sub>SRCas</sub>	Stable	0.77	7.64	0.69	43.82	-2.10	959
			Unstable	0.91	9.50	0.84	64.12	0.94	709
			All	0.90	9.92	0.93	53.40	0.98	1668
	(Rn-G) <sub>SRShap</sub>	(H + LE) <sub>SRShap</sub>	Stable	1.04	-9.00	0.63	61.62	2.84	202
			Unstable	0.90	-1.80	0.50	123.21	0.90	196
			All	0.93	-10.17	0.80	96.97	0.87	398

with previous  $SR_{Cas}$  results reported in publications by Castellví et al. (2006, 2008). Thus,  $SR_{Cas}$  and  $SR_{Shap}$  results can be considered as reasonably reliable, although  $SR_{Shap}$  dataset was limited by the size of the experimental set. The parameter  $D$  should be taken cautiously as it might compensate errors for the sums it uses in calculation. Also, it may lead to confusion when the periods under stable atmospheric conditions are evaluated; as the difference  $Rn-G$  and the sum  $LE + H$  are often different in sign which have resulted in few negative  $D$  values (Table 5). The dew formation may also disturb the sign of data as it is followed by negative  $LE$ . Other statistical parameters listed in Table 5 are useful for broader comparison between the reference method (EC) and the new methods ( $SR_{Cas}$  and  $SR_{Shap}$ ). For example, the slopes were closer to unity in all cases for SR, but intercepts were slightly worse when energy balance is

estimated. Two more considerations should be mentioned. Firstly, the root square mean error, RSME, in  $H_{EC}$  comparison for different brands of EC systems obtained in ideal conditions over short, dense and homogeneous vegetation is found to range between 6.1 and 21  $W m^{-1}$  (Twine et al., 2000; Mauder et al., 2007). Secondly, the lack of sonic anemometer to "sense" mean vertical wind velocities of very small magnitudes ( $0.001 m s^{-1}$ ) influences EC results to be underestimates of actual fluxes. It is unknown how a non-zero mean vertical velocity may affect the SR method, but it likely has less impact than in the EC method. Namely, a non-zero  $\bar{w}$  might cause an underestimate of the actual flux in SR analysis because it assumes that there is no mass or heat loss through the air parcel top, but the mean vertical displacement of the scalar, while the air parcel is connected to the surface is negligible when compared

with the air parcel height ( $\sim 6.9$  m in our case). The corresponding error is on the order of  $10^{-2}$ , which is within the instrumental measurement error for vertical placement above the ground (Castellví et al., 2008).

In this study,  $SR_{Cas}$  approach generally performed well under both stable and unstable conditions, given that the energy balance closure and its components were in agreement with the EC results (Fig. 5).  $SR_{Shap}$  have shown similar performance for energy balance closure to EC and  $SR_{Cas}$ , according to values for  $D$  statistics, under unstable and all stability conditions.  $R^2$  are lower than the ones obtained for EC or  $SR_{Cas}$ . There was more scatter in case of the late peaches (ST1) observed for all methods and less scatter in EC results than in  $SR_{Cas}$  or  $SR_{Shap}$  for both maturing peach types. Energy balance is, in general, overestimated by all methods for low available energy (Rn-G) values (Fig. 5). For higher values of available energy, the turbulent fluxes are, mostly, underestimated. The crossing value between under- and overestimation of available energy, i.e. where estimated fluxes can close the energy balance equation are found around: (1)  $50 \text{ W m}^{-2}$  (EC-ST1), (2)  $100 \text{ W m}^{-2}$  ( $SR_{Cas}$ -ST1), (3)  $100 \text{ W m}^{-2}$  ( $SR_{Shap}$ -ST1), (4)  $0 \text{ W m}^{-2}$  (EC-ST2), (5)  $20 \text{ W m}^{-2}$  ( $SR_{Cas}$ -ST2), (6) no overestimation is observed ( $SR_{Shap}$ -ST2). Those values are characteristic for the neutral atmospheric conditions in the early morning or the late afternoon. Generally the agreement between  $H + LE$  and Rn-G was better for early morning than for late afternoon hours although the flux underestimation was common phenomenon for the micrometeorological methods. Additionally, it was noticed that for great evaporative demand, LE values were very high, but  $H + LE$  almost never reached energy balance closure. As a consequence of all the uncertainties that are related to the EC method, the regression analysis resulted in the slopes significantly different from 1.0 and the intercepts significantly different from 0.0 (level of significance equal to 0.05).

All the calculated statistics indicators (slope, intercept,  $R^2$ , RMSE and  $D$ ) of the data quality better performed for the energy balance closure obtained at the ST2 (Table 5). Also, there was a higher agreement between EC and  $SR_{Cas}$  results for this site (Table 4). For  $SR_{Shap}$   $R^2$  results were not very consistent (Table 4). The conditions for micrometeorological measurements seemed to be more favorable at the station ST2. There are a few possible explanations for this kind of behavior, including the terrain complexity over the surface considered for the measurement footprint. As it can be seen

in Fig. 2 the terrain close to ST1 is sloping down from the measurement spot, at 150 m height, to the fetch limit, at 130 m height above mean sea level. There is also a hilly zone that is limiting a part of footprint flux contribution at both ST1 and ST2 which was the reason to decide to stay only with those periods when the wind direction was between  $\pm 45^\circ$  of the CSAT3 orientation angle. In the ST2 case, sloping down is towards the point where the measurements were set, at 120 m above the mean sea level. Gradual rise of the terrain occurs in the direction of the fetch limit, at 150 m above the mean sea level. It seems that this change in the terrain leveling can influence the EC method performance and therefore also the SR. Namely, the CSAT3 is sensitive to the complex terrain issues and thus limits the accuracy of the methods depending on such measurements. According to Baldocchi et al. (2000) advection of mass and energy can occur in circumstances when the underlying surface is heterogeneous. The cases where it can be expected more often are sites with different roughness or different source/sink strength transitions such as between forests and crops, vegetation and lakes, and desert and irrigated crops (Rao et al., 1974; Bink, 1996; Sun et al., 1997). Unfortunately we did not have any measurement equipment set that would describe the possibility of advection. Another possible cause of differences between the two sites is the tree plantation design. As it is a heterogeneous crop plantation, the larger distances in tree plantation both between rows and the tree trunks in the row for the ST1 might be of importance. More contribution to the scalar fluxes by the understory vegetation is expected in orchards with more widely spaced trees, further contributing to the surface heterogeneity.

Here, we have used the simplified energy balance equation, while  $F_p$  was ignored for lack of adequate equipment. Improving the precision in estimating  $H + LE + F_p$  according to the appropriate method and representative surface with sufficient fetch has a long-term impact on analyzing the watershed management for agricultural use, carbon sequestration, and climate model validations and calibrations (Oncley et al., 2007; Baldocchi et al., 2004). Castellví et al. (2008) neglected  $F_p$  from energy balance equation, stating that estimation of this variable in rangeland grass were negligible ( $-14 \text{ W m}^{-2} < F_p < 5 \text{ W m}^{-2}$ ). However,  $F_p$  might explain some part of the flux loss in the sparse, moderately tall canopies.

Our results are confirming that there is no need for calibration of  $SR_{Cas}$  against another method to obtain accurate LE data (and

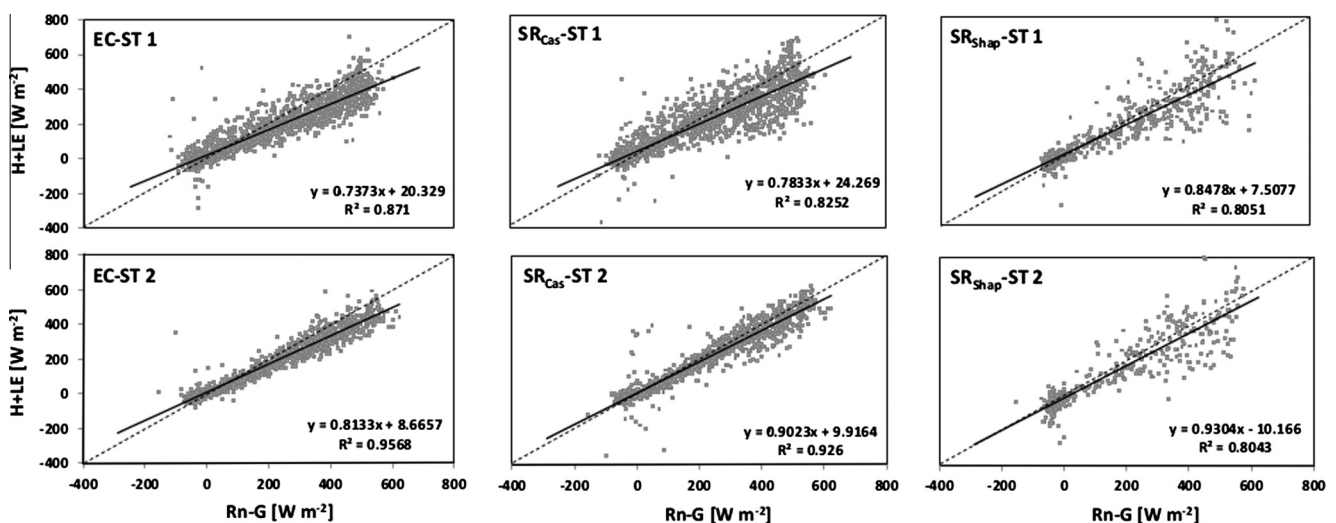


Fig. 5. Measured available energy (net radiation minus soil heat flux, Rn-G) versus estimated scalar fluxes (sensible and latent heat flux,  $LE + H$ ) for both stations and methods used. ST1, late peaches; ST2, early peaches; EC, eddy covariance; SR, surface renewal following the Castellví approach (Castellví, 2004; Castellví et al., 2006, 2008). The data presented is for the whole measuring period and all stability atmospheric conditions.

ET estimates) even in heterogeneous canopies.  $SR_{Shap}$  method performed relatively well, with  $\alpha$  values close to 1.00 for unstable cases, which proves the importance of distinguishing between different ramp scales. It may be that even larger ramp scales, and not the detected Scale One or Scale Two, are relevant to surface-layer fluxes during stable conditions. If this is the case, more research is needed to develop methods for determining the number of ramp scales in a time series and which scale is important for the flux.

Following Castellví (2004) there are two options for measurement sets to meet the needs for data collection for the presented auto-calibration SR method: (1) to have only high frequency temperature measurements and mean wind velocity; and (2) to have high frequency measurements of both temperature and wind velocity. As we deployed EC equipment, we suffered a great amount of data loss because of the CSAT3 orientation needs, fetch requirements for proper EC operation, and the  $SR_{Cas}$  and  $SR_{Shap}$  calculation procedures itself; thus we believe that the  $SR_{Cas}$  and  $SR_{Shap}$  methods did not completely show its potential performance in this work because some of the uncertainties and shortcomings of the EC method should have affected the SR analyses, too. We could expect at least similar results in those experimental layouts where fine-wire thermocouples are used with cup anemometer, thus reducing minimum fetch limits and avoiding some of the above mentioned problems (Castellví, 2012). This may lead to more confidence in applying fine-wire thermocouples alone or together with high-frequency measurements of water vapor density when applying  $SR_{Cas}$  analysis. In that case cup anemometer would be necessary in deriving some parameters such as Obukhov length and friction velocity.  $SR_{Shap}$  method should be validated more to be applied independently for ET estimation.

#### 4. Conclusions

When considering all stability conditions together, energy imbalance for  $SR_{Cas}$  results, expressed in terms of the statistics  $D$ , was quite good, about 2–6%, while the  $D$  statistics for the imbalance for  $SR_{Shap}$  was similar to EC, about 13%. Taking into account together the different statistics,  $D$ , slope, intercept and RMSE, we can state that  $SR_{Cas}$  has shown similar or only slightly better energy balance closures.  $SR_{Shap}$  has shown similar tendency like  $SR_{Cas}$  but the performance was slightly poorer. It should be tested in future because of the limited number of data points it yielded for our measurement set and for the calculation procedure itself. However it has shown that the same principles apply in the sparse heterogeneous crop as earlier shown in short homogenous or bare soil. It also showed potential application in LE estimation.

A good correlation between turbulent fluxes obtained by EC and  $SR_{Cas}$  ('all stability periods' and 'unstable periods' cases) was found (with  $R^2$  ranging between 0.82 and 1.00). For the same atmospheric conditions, the analysis of turbulent fluxes estimated by EC and  $SR_{Shap}$  showed good correlation (with corresponding values ranging between 0.49 and 0.79). Better correlation is observed in  $H$  fluxes comparison. Shapland et al. (2012b) published results that show better correlation for unstable than stable cases for  $H$  calculation. We have noticed that  $LE_{SR_{Shap}}$  to  $LE_{EC}$  comparison resulted in higher  $R^2$  values for stable than unstable conditions.

Some overestimation in fluxes determined by  $SR_{Cas}$  was noticed in agreement with earlier published works in homogeneous canopies. Expressing the RMSE values from Table 4 in terms of water depth (ET), the average uncertainty of the SR methods compared to the EC method was very small, around  $0.07 \text{ mm h}^{-1}$  for  $SR_{Cas}$  and around  $0.11 \text{ mm h}^{-1}$  for  $SR_{Shap}$ . These results confirmed the auto-calibration feature of the  $SR_{Cas}$  and  $SR_{Shap}$  method according to atmospheric stability conditions despite that some lack of

similarity for temperature and water vapor exchange is possible under stable atmospheric conditions.

In summary we suggest usefulness of the methods  $SR_{Cas}$  and  $SR_{Shap}$  as interesting alternatives to the EC for the irrigation management in heterogeneous crop for its high performance in statistical comparison and due to demonstrated independency of operation.

#### Acknowledgments

Work funded by the project Consolider CSD2006 – 00067 (Ministerio de Ciencia e Innovación, Spain). Thanks are due to the owners of the commercial orchard, to J.L. Gracia (farm manager), M. Izquierdo, J. Gaudó, J.M. Acín, E. Medina, and C. Merino for technical and field assistance; and to the manuscript reviewers for their useful comments.

#### References

- Allen, R.G., Pruitt, W.O., Businger, J.A., Fritschen, L.J., Jensen, M.E., Quinn, F.H., 1996. Evaporation and transpiration. In: Heggen, R.J., Wootton, T.P., Cecilio, C.B., Fowler, L.C., Hui, S.L. (Eds.), *Hydrology Handbook*, second ed. American Society of Civil Engineers, New York, pp. 125–252.
- Antonia, R.A., Rajagopalan, A., Chambers, A.J., 1983. Conditional sampling of turbulence in the atmospheric surface layer. *J. Clim. Appl. Meteorol.* 22, 69–78.
- Baldocchi, D.D., Finnigan, J.J., Wilson, K.W., et al., 2000. On measuring net ecosystem carbon exchange in complex terrain over tall vegetation. *Bound. Layer Meteorol.* 96, 257–291.
- Baldocchi, D.D., Liukang, X., Kiang, N., 2004. How plant functional-type, weather, seasonal drought, and soil physical properties alter water and energy fluxes of an oak-grass savanna and an annual grassland. *Agric. For. Meteorol.* 123, 13–39.
- Bink, N.J., 1996. The Structure of the Atmospheric Surface Layer Subject to Local Advection, PhD thesis. Agricultural University, Wageningen, The Netherlands.
- Campbell Scientific, 1996. Eddy covariance system operator's manual CA27 and KH20, Revision 9/96. Campbell Scientific, Inc. Logan.
- Castellví, F., 2004. Combining surface renewal analysis and similarity theory: a new approach for estimating sensible heat flux. *Water Resour. Res.* 40, W05201. <http://dx.doi.org/10.1029/2003WR002677>.
- Castellví, F., 2012. Fetch requirements using surface renewal analysis for estimating scalar surface fluxes from measurements in the inertial sublayer. *Agric. For. Meteorol.* 152, 233–239.
- Castellví, F., Martínez-Cob, A., 2005. Estimating sensible heat flux using surface renewal analysis and flux variance method: a case study over olive trees at Sagtogo (NE of Spain). *Water Resour. Res.* 41, W09422, 1–10.
- Castellví, F., Snyder, R.L., 2009a. On the performance of surface renewal analysis to estimate sensible heat flux over two growing rice fields under the influence of regional advection. *J. Hydrol.* 375, 546–553.
- Castellví, F., Snyder, R.L., 2009b. Sensible heat flux estimates using surface renewal analysis. A study case over peach orchard. *Agric. For. Meteorol.* 149, 1397–1402.
- Castellví, F., Snyder, R.L., 2010. A comparison between latent heat fluxes over grass using a weighing lysimeter and surface renewal analysis. *J. Hydrol.* 381, 213–220.
- Castellví, F., Martínez-Cob, A., Pérez-Coveta, O., 2006. Estimating sensible and latent heat fluxes over rice using surface renewal. *Agric. For. Meteorol.* 139, 164–169.
- Castellví, F., Snyder, R.L., Baldocchi, D.D., 2008. Surface energy-balance closure over rangeland grass using the eddy covariance method and surface renewal analysis. *Agric. For. Meteorol.* 148, 1147–1160.
- Chen, W., Novak, M.D., Black, T.A., Lee, X., 1997a. Coherent eddies and temperature structure functions for three contrasting surfaces. Part I: Ramp model with finite micro-front time. *Bound-Lay. Meteorol.* 84, 99–123.
- Chen, W., Novak, M.D., Black, T.A., Lee, X., 1997b. Coherent eddies and temperature structure functions for three contrasting surfaces. Part II: Renewal model for sensible heat flux. *Bound. Layer Meteorol.* 84, 125–147.
- Collineau, S., Brunet, Y., 1993. Detection of turbulent coherent motions in a forest canopy. Part II: Time-scales and conditional averages. *Bound. Layer Meteorol.* 66, 49–73.
- Collineau, S., Brunet, Y., 1993. Detection of turbulent coherent motions in a forest canopy. Part II: Time-scales and conditional averages. *Boundary-Layer Meteorol.* 66, 1993, 49–73.
- Duce, P., Spano, D., Snyder, R.L., 1998. Effect of different fine wire thermocouple design on high frequency temperature measurement. In: 23rd Conference on Agricultural and Forest Meteorology, Albuquerque, New Mexico, USA, November 2–6, 1998, pp. 146–147.
- Foken, T., 2006. 50 years of the Monin-Obukhov similarity theory. *Boundary-Layer Meteorol.* 119, 431–447.
- Gao, W., Shaw, R.H., Paw U, K.T., 1989. Observation of organized structure in turbulent flow within and above a forest canopy. *Bound. Layer Meteorol.* 47, 349–377.
- Högström, U., 1988. Non-dimensional wind and temperature profiles in the atmospheric surface layer; a re-evaluation. *Bound. Lay. Meteorol.* 42, 55–78.

- Jamieson, P.D., Porter, J.R., Goudriaan, J., Ritchie, J.T., van Keulen, H., Stol, W., 1998. A comparison of the models AFRCWHEAT2, CERES-Wheat, Sirius, SUCROS2 and SWHEAT with measurements from wheat grown under drought. *Field Crops Res.* 55, 23–44.
- Katul, G., Hsieh, C., Oren, R., Ellsworth, D., Philips, N., 1996. Latent and sensible heat flux predictions from a uniform pine forest using surface renewal and flux variance methods. *Boundary Layer Meteorol.* 80, 249–282.
- Kustas, W.P., Prueger, J.R., Humes, K.S., Starks, P.J., 1999. Estimation of surface heat fluxes at field scale using surface layer versus mixed layer atmospheric variables with radiometric temperature observations. *J. Appl. Meteorol.* 38, 224–238.
- Mahrt, L., 1998. Flux sampling errors for aircraft and towers. *J. Atmos. Oceanic Technol.* 15, 416–429.
- Martínez-Cob, A., Faci, J.M., 2010. Evapotranspiration of a hedge-pruned olive orchard in a semiarid area of NE Spain. *Agric. Water Manage.* 97, 410–418.
- Martínez-Cob, A., Zapata, N., Sánchez, I., 2010. Viento y Riego: la variabilidad del viento en Aragón y su influencia en el riego por aspersión. Publication No. 2948. Series Studies (Geography). Institución Fernando el Católico. Zaragoza, Spain. 200 pp. [in Spanish].
- Mauder, M., Oncley, S.P., Vogt, R., Weidinger, T., Ribeiro, L., Bernhofer, C., Foken, T., Kosiek, W., De Bruin, H.A.R., Liu, H., 2007. The energy balance experiment EBEX-2000. Part II: Intercomparison of eddy-covariance sensors and post-field data processing methods. *Bound. Layer Meteorol.* 123, 29–54.
- Oncley, S.P., Foken, T., Vogt, R., Kohsiek, W., DeBruin, H.A.R., Bernhofer, C., Christen, A., Van Gorsen, E., Grantz, D., Feigenwinter, C., Lehner, I., Liebethal, C., Liu, H., Mauder, M., Pitacco, A., Ribeiro, L., Weidinger, T., 2007. The energy balance experiment EBEX-2000. Part I: overview and energy balance. *Bound. Layer Meteorol.* 123, 1–28.
- Paw U, K.T., Qiu, J., Su, H.B., Watanabe, T., Brunet, Y., 1995. Surface renewal analysis: a new method to obtain scalar fluxes without velocity data. *Agric. For. Meteorol.* 74, 119–137.
- Paw U, K.T., Snyder, R.L., Spano, D., Su, H.B., 2005. Surface renewal estimates of scalar exchanges. *Micrometeorology in Agricultural Systems, Agron. Monogr.*, vol. 47, pp. 445–484, ASA-CSSA-SSSA, Madison, Wisc.
- R Development Core Team, 2012. R: A language and environment for statistical computing. R Foundation for Statistical Computing, Vienna, Austria, ISBN-900051-07-0.
- Rao, K.S., Wyngaard, J.C., Cote, O.R., 1974. Local advection of momentum, heat, and moisture in micrometeorology. *Bound. Layer Meteorol.* 7, 331–348.
- Sellers, P.J., Mintz, Y., Sud, Y.C., Dalcher, A., 1986. A simple biosphere model (SiB) for use within general circulation models. *J. Atmos. Sci.* 43, 505–531.
- Shapland, T.M., McElrone, A.J., Snyder, R.L., Paw U, K.T., 2012a. Structure function analysis of two-scale scalar ramps. Part I: theory and modelling. *Bound. Layer Meteorol.* 145, 5–25. <http://dx.doi.org/10.1007/s10546-012-9742-5>.
- Shapland, T.M., McElrone, A.J., Snyder, R.L., Paw U, K.T., 2012b. Structure function analysis of two-scale scalar ramps. Part II: ramp characteristics and surface renewal flux estimation. *Bound. Layer Meteorol.* 145, 27–44. <http://dx.doi.org/10.1007/s10546-012-9740-7>.
- Snyder, R.L., Spano, D., Paw U, K.T., 1996. Surface renewal analysis for sensible and latent heat flux density. *Bound. Layer Meteorol.* 77, 249–266.
- Spano, D., Snyder, R.L., Duce, P., Paw U, K.T., 1997. Surface renewal analysis for sensible heat flux density using structure functions. *Agric. For. Meteorol.* 86, 259–271.
- Spano, D., Snyder, R.L., Duce, P., Paw U, K.T., 2000. Estimating sensible and latent heat flux densities from grapevine canopies using surface renewal. *Agric. For. Meteorol.* 104, 171–183.
- Stull, R.B., 1988. *An Introduction to Boundary Layer Meteorology*. Kluwer Academic (666 pp.).
- Sun, J., Lenschow, D.H., Mahrt, L., Crawford, D.L., Davis, K.J., Oncley, S.P., MacPherson, J.I., Wang, Q., Dobosy, R.J., Desjardins, R.L., 1997. Lake-induced atmospheric circulations during BOREAS. *J. Geophys. Res.* 102, 29155–29166.
- Twine, T.E., Kustas, W.P., Norman, J.M., Cook, D.R., Houser, P.R., Meyers, T.P., Prueger, J.H., Starks, P.J., Wesely, M.L., 2000. Correcting eddy-covariance flux underestimates over a grassland. *Agric. For. Meteorol.* 103, 279–300.
- Van Atta, C.W., 1977. Effect of coherent structures on structure functions of temperature in the atmospheric boundary layer. *Arch. Mech.* 29, 161–171.
- Webb, E.K., Pearman, G.I., Leuning, R., 1980. Correction of flux measurements for density effects due to heat and water vapour transfer. *Quart. J. Roy. Meteorol. Soc.* 106, 85–100.
- Wilson, K., Goldstein, A., Falge, E., Aubinet, M., Baldocchi, D., Bernbigler, P., Bernhofer, C., Ceulemans, R., Dolman, H., Field, C., Grelle, A., Ibrom, A., Law, B.E., Kowalski, A., Meyers, T., Moncrieff, J., Monson, R., Oechel, W., Tenhunen, J., Valentini, R., Verma, S., 2002. Energy balance closure at FLUXNET sites, vol. 113, pp. 223–243.
- Zapata, N., Martínez-Cob, A., 2001. Estimation of sensible and latent heat flux from natural sparse vegetation surfaces using surface renewal. *J. Hydrol.* 254, 215–228.
- Zapata, N., Nerilli, E., Martínez-Cob, A., Chalhaf, I., Chalhaf, B., Fliman, D., Playán, E., 2013. Limitations to adopting regulated deficit irrigation in stone fruit orchards: a case study. *Span. J. Agric. Res.* 11, 529–546.
- Zhao, X., Liu, Y., Tanaka, H., Hiyama, T., 2010. A comparison of flux variance and surface renewal methods with eddy covariance. *IEEE J. Selected Top. Appl. Earth Observ. Remote Sens.* 3, 345–350. <http://dx.doi.org/10.1109/JSTARS.2010.2060473>.